JOC Article
pubs.acs.org/joc

Versatile $^{1}H-^{31}P-^{31}P$ COSY 2D NMR Techniques for the Characterization of Polyphosphorylated Small Molecules

Ananya Majumdar,[†] Yan Sun,[‡] Meha Shah,[‡] and Caren L. Freel Meyers*,[‡]

[†]*The Johns Hopkins University Biomolecular NMR Center and* [‡]*Department of Pharmacology, Johns Hopkins School of Medicine, Baltimore, Maryland 21205*

cmeyers@jhmi.edu

Received January 14, 2010

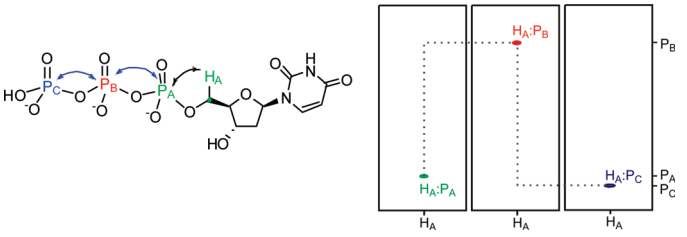

Di- and triphosphorylated small molecules represent key intermediates in a wide range of biological and chemical processes. The importance of polyphosphorylated species in biology and medicine underscores the need to develop methods for the detection and characterization of this compound class. We have reported two-dimensional HPP-COSY spectroscopy techniques to identify diphosphate-containing metabolic intermediates at submillimolar concentrations in the methylerythritol phosphate (MEP) isoprenoid biosynthetic pathway.[1] In this work, we explore the scope of HPP-COSY-based techniques to characterize a diverse group of small organic molecules bearing di- and triphosphorylated moieties. These include molecules containing P−O−P and P−C−P connectivities, multivalent P(III)−O−P(V) phosphorus nuclei with widely separated chemical shifts, as well as virtually overlapping ^{31}P resonances exhibiting strong coupling effects. We also demonstrate the utility of these experiments to rapidly distinguish between mono- and diphosphates. A detailed protocol for optimizing these experiments to achieve best performance is presented.

Introduction

Polyphosphorylated compounds are ubiquitous in Nature and are essential for numerous biological processes. Nucleotides, the most abundant polyphosphorylated natural products, serve as building blocks in DNA and RNA biosynthesis. In addition, these naturally occurring polyphosphorylated compounds play key roles in metabolism, acting as energy sources (ATP and GTP) and performing important roles as cofactors in many biochemical processes (CoA, NADH, etc.). In medicine, nucleoside diphosphates and triphosphates are the active metabolites of a variety of cytotoxic nucleoside anticancer and antiviral agents.[2,3] Bisphosphonates are stable diphosphate analogues with applications in organometallic chemistry and medicine[4−11] and as chemical probes in biological processes.[12,13]

The detection and/or characterization of polyphosphorylated molecules poses particular challenges in chemistry and

(1) Majumdar, A.; Shah, M. H.; Kipchirchir Bitok, J.; Hassis-LeBeau, M. E.; Meyers, C. L. F. *Mol. BioSyst.* **2009**, *5*, 935–944.
(2) Salas-Alvarez, L. M. *Curr. Top. Med. Chem.* **2008**, *8*, 1379–1404.
(3) De Clercq, E. *Rev. Med. Virol.* **2009**, *19*, 287–299.
(4) Reid, I. R. *Sem. Cell Dev. Biol.* **2008**, *19*, 473–478.
(5) Russell, R. G. *Ann. N.Y. Acad. Sci.* **2006**, *1068*, 367–401.
(6) Winter, M. C.; Coleman, R. E. *Curr. Opin. Oncol.* **2009**, *21*, 499–506.
(7) Husaini, H. A.; Wheatly-Price, P.; Clemons, M.; Shepherd, F. A. *J. Thoracic Oncol.* **2009**, *4*, 251–259.
(8) Li, Y.-Y.; Chang, J. W.; Chou, W.-C.; Liaw, C.-C.; Wang, H.-M.; Huang, J.-S.; Wang, C.-H.; Yeh, K.-Y. s. *Lung Cancer* **2008**, *59*, 180–191.
(9) Zhang, Y.; Leon, A.; Song, Y.; Studer, D.; Haase, C.; Koscielski, L. A.; Oldfield, E. *J. Med. Chem.* **2006**, *49*, 5804–5814.
(10) Martin, M. B.; Grimley, J. S.; Lewis, v. C.; Heath, H. T., III; Bailey, B. N.; Kendrick, H.; Yardley, V.; Caldera, A.; Lira, R.; Urbina, J. A.; Moreno, S. N. J.; Docampo, R.; Croft, S. L.; Oldfield, E. *J. Med. Chem.* **2001**, *44*, 909–916.
(11) Leon, A.; Liu, L.; Yang, v.; Hudock, M. P.; Hall, P.; Yin, F.; Studer, D.; Puan, K.-J.; Morita, C. T.; Oldfield, E. *J. Med. Chem.* **2006**, *49*, 7331–7341.
(12) Joseph, S. M.; Pifer, M. A.; Przybylski, R. J.; Dubyak, G. R. *Br. J. Pharmacol.* **2004**, *142*, 1002–1014.
(13) Zhang, Y.; el Kouni, M. H.; Ealick, S. E. *Acta Crystallogr.* **2007**, *D63*, 126–134.

Published on Web 04/22/2010 DOI: 10.1021/jo100042m

biology. The characterization of ^{31}P nuclei in these compounds by NMR has traditionally been accomplished by direct, one-dimensional ^{31}P NMR, often at low magnetic field strengths on relatively concentrated samples (typically >50 mM). Complex systems containing multiple ^{31}P sites or a mix of mono- and diphosphate centers require more detailed and unambiguous characterization, which is hampered at low concentrations. Furthermore, reaction mixtures containing multiple phosphorylated compounds are difficult to characterize given the difficulties in making accurate assignments to ^{31}P resonances in individual polyphosphorylated species. These difficulties can be addressed by using two-dimensional, indirect ^{1}H detected techniques, which correlate ^{31}P centers in the molecule to covalently linked protons. Not only does this increase the information context of the spectrum but also potentially benefits from the high sensitivity of ^{1}H excitation and detection experiments. These experiments may be adapted from the repertoire of HSQC,[14,15] HMQC,[16] or HMBC[17] techniques that are available for ^{13}C and ^{15}N characterization. In contrast to ^{1}H$-^{13}$C and ^{1}H$-^{15}$N experiments, which require either isotope labeling or, for natural abundance studies, highly sensitive probes and high sample concentration, ^{1}H$-^{31}$P experiments benefit from the nearly 100% natural abundance of ^{31}P.

Despite these potential advantages, ^{1}H$-^{31}$P experiments are underutilized. Since the sensitivity of ^{1}H-X (X = ^{13}C, ^{15}N, etc) correlated experiments is proportional to the strength of the appropriate J_{HX} coupling constant, the large and relatively uniform $^{1}J_{HC}$ and $^{1}J_{HN}$ coupling constants result in high sensitivity in ^{1}H$-^{13}$C and ^{1}H$-^{15}$N correlation spectra under conditions of isotopic enrichment (or high concentrations at natural abundance). However, most ^{1}H$-^{31}$P experiments do not offer this advantage. Although one-bond $^{1}J_{HP}$ coupling constants are large (>600 Hz), typical phosphorus-containing compounds only possess multiple-bond $^{n}J_{HP}$ couplings (often through H$-$C$-$O$-$P linkages) which are significantly smaller (<20 Hz) and highly variable due to dependence on local geometry. As a result, ^{1}H$-^{31}$P HSQC and related experiments have not been widely used for the characterization of small molecules containing ^{31}P nuclei.

A growing need for detecting ^{31}P containing compounds at *low concentrations* revives interest in ^{1}H-detected, multidimensional ^{31}P NMR. This has been facilitated by the ever increasing sensitivity of NMR probes for ^{1}H detection, including the availability of cryogenic probes. On modern spectrometers, even on room-temperature probes, low millimolar to submillimolar levels of ^{31}P-containing low molecular weight compounds may be detected using ^{1}H-detected techniques, as long as the $J_{HP} \geq 5$ Hz.[18−21]

We have found the sensitivity of ^{1}H-detected ^{31}P experiments to be especially advantageous when applied to polyphosphorylated compounds.[1] In 1D ^{31}P NMR spectra, di- and triphosphates with distinct chemical shifts, are usually identified by splittings due to $^{n}J_{PP}$ coupling constants. However, more detailed and unambiguous structural characterization is often required and may be obtained from ^{1}H$-^{31}$P$-^{31}$P COSY spectra, in which ^{31}P$-^{31}$P COSY cross peaks are correlated to relevant protons through J_{HP} couplings. These experiments are particularly useful for distinguishing "open" (^{1}H$-^{31}$P$-^{31}$P) species relative to "bounded" (^{1}H$-^{31}$P$-^{31}$P$-^{1}$H) "coupling networks", or for characterizing structural (conformational) rearrangements in which the identities of the coupled ^{1}H or ^{31}P partners are changed. The large (>20 Hz) and fairly uniform ^{31}P$-^{31}$P coupling constants exhibited by polyphosphorylated compounds facilitates high sensitivity in ^{1}H detected, ^{1}H$-^{31}$P$-^{31}$P 2D NMR experiments for detailed structural information at low concentrations. Recently, we have used this technique very effectively to characterize and discriminate a series of diphosphate-containing intermediates produced enzymatically in the nonmammalian MEP pathway for isoprenoid biosynthesis. Using HPP-COSY techniques, we demonstrated these enzymatic reactions could be studied in situ at low substrate concentrations (<3 mM) without the need for isotopic enrichment or purification.[1] The success of this approach for the characterization of MEP pathway intermediates highlights the potential value of HPP-COSY techniques as structure determination tools for the organic chemist and has prompted us to explore the scope and limitations of these techniques for characterization of other structurally diverse phosphorylated small molecules.

Here, we report and discuss applications of HP-HSQC- and HPP-COSY-based techniques to a variety of phosphorylated small molecules to illustrate the applicability of these experiments. We have highlighted seven compounds (**1**−**7**, Figure 1) in order to demonstrate HP-NMR techniques for the characterization of biologically and chemically relevant molecules exhibiting various distinguishing features, such as the presence of a P$-$C$-$P linkage (**2**), large differences in ^{31}P chemical shift (**3**), overlapping, strongly coupled ^{31}P nuclei (**4**), and triphosphate (**6**, **7**) linkages. Finally, we provide a practical guide for the execution of experiments, such that HPP-COSY experiments can be used successfully at low millimolar or even submillimolar concentrations relevant in many chemical and biological systems.

Results

Theory. The ^{1}H$-^{31}$P and ^{1}H$-^{31}$P$-^{31}$P pulse sequences used in this work have been published elsewhere[1] but have been reproduced in Figure S1 (see the Supporting Information) for the sake of clarity. The ^{1}H$-^{31}$P correlation experiments are essentially HSQC and constant-time (CT) HSQC experiments (see the Supporting Information for theoretical and experimental details). We refer to the relevant network of J-coupled nuclei as $H_A-P_A-P_B-H_B$, where H_A:P_A and H_B:P_B are correlated by $^{n}J_{HP}$ coupling constants (n may be different for H_A:P_A and H_B:P_B) and P_A:P_B are coupled via a $^{2}J_{PP}$ coupling constant (see Figure 2). Note that P_A and P_B refer to ^{31}P nuclei whose chemical shifts are distinct and magnetically and chemically nonequivalent.

(14) Bax, A.; Griffey, R. H.; Hawkins, B. L. J. *J. Magn. Reson.* **1983**, *55*, 301–315.
(15) Bax, A.; Subramanian, S. *J. Magn. Reson.* **1986**, *67*, 565–569.
(16) Bodenhausen, G.; Ruben, D. J. *Chem. Phys. Lett.* **1980**, *69*, 185–189.
(17) Bax, A.; Summers, M. F. *J. Am. Chem. Soc.* **1986**, *108*, 2093–2094.
(18) Albaret, C.; Loeillet, D.; Auge, P.; Pierre-Louis, F. *Anal. Chem.* **1997**, *69*, 2694–2700.
(19) Gradwell, M. J.; Fan, T. W.; Lane, A. N. *Anal. Biochem.* **1998**, *263*, 139–149.
(20) Larijani, B.; Poccia, D. L.; Dickinson, L. C. *Lipids* **2000**, *35*, 1289–1297.
(21) Petzold, K.; Olofsson, A.; Arnqvist, A.; Gröbner, G.; Schleucher, J. *J. Am. Chem. Soc.* **2009**, *131*, 14150–14151.

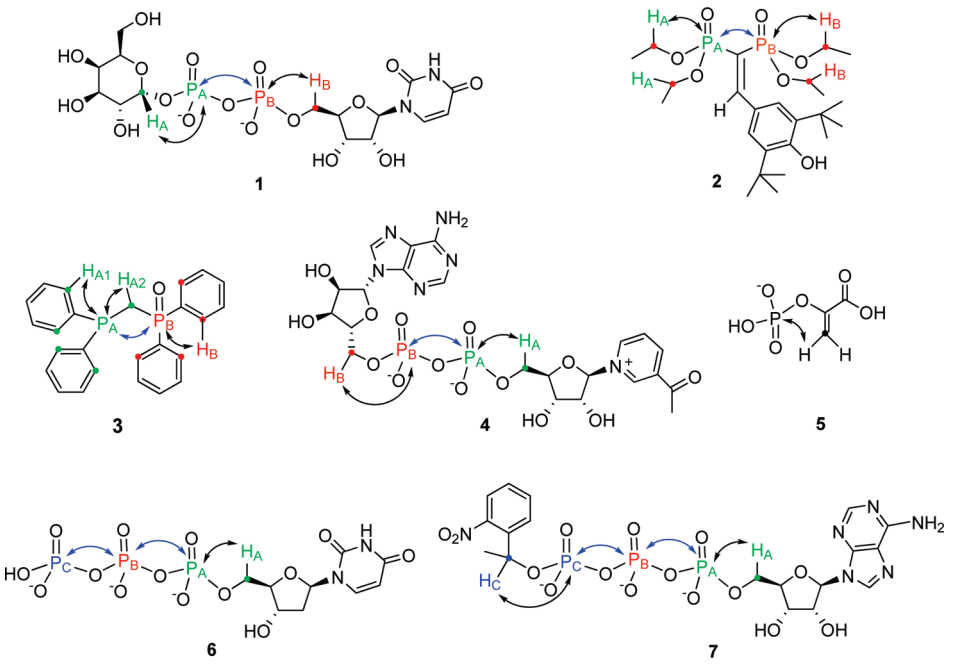

FIGURE 1. Structures of compounds highlighted for the HP NMR studies: UDP-galactose (**1**), *P*,*P*′-[[3,5-bis(1,1-dimethylethyl)-4-hydroxyphenyl]ethenylidene]bis-*P*,*P*,*P*′,*P*′-tetraethyl ester (**2**), bis(diphenylphosphine)methane monooxide (dppmO) (**3**), nicotinamide adenine dinucleotide (NAD^+) (**4**), phosphoenol pyruvate (PEP) (**5**), dUTP (**6**), adenosine 5′-triphosphate, P^3-1-(2-nitrophenyl)ethyl ester (caged ATP analogue) (**7**). The carbons with attached protons coupled to ^{31}P nuclei are represented by dots. Some protons are omitted on these carbons for clarity. The coupling networks are shown by arrows (black, $^1H-^{31}P$ coupling; blue, $^{31}P-^{31}P$ coupling). These ^{31}P-containing compounds display distinguishing structural features. In compound **2**, a P−C−P linkage replaces the more commonly found P−O−P linkage. Compound **3** bears two ^{31}P nuclei exhibiting a large ^{31}P chemical shift difference. In contrast, the two ^{31}P nuclei in compound **4** exhibit a very small chemical shift difference (Δppm ~0.3 ppm). Compound **6** bears an additional P−O−P in its triphosphate linkage. Each of these compound classes imposes distinct challenges for H,P NMR characterization techniques, demonstrating the scope of these experiments for the characterization of phosphorylated small molecules.

In an $^1H-^{31}P$ HSQC spectrum of an $H_A-P_A-P_B-H_B$ spin system, the presence of a coupling constant between H_A and P_A and between H_B and P_B, results in the observation of cross peaks H_A:P_A (correlation between the chemical shift frequencies of H_A along the ^1H dimension and P_A along the ^{31}P dimension) and H_B:P_B (Figure 2a). The intensity of the cross peaks (and hence, the sensitivity of the spectrum) is proportional to the strength of the appropriate coupling constant $^nJ_{HP}$ (where *n* is the number of intervening bonds between ^1H and ^{31}P). When the ^{31}P dimension is acquired in high resolution, the H_A:P_A and H_B:P_B cross peaks are split into doublets along the ^{31}P axis by $^2J_{PP}$. In comparison, in an isolated H_C-P_C spin system (monophosphate) where P_C is not coupled to a second ^{31}P nucleus, the observed cross peak H_C:P_C remains a singlet. This is shown schematically in Figure 2a.

The observed splitting of the P_A and P_B resonances into doublets indicates that they belong to a diphosphate species. However, establishing that P_A and P_B are coupled to *each other* requires a $^{31}P-^{31}P$ 2D COSY experiment, where the $^2J_{PP}$ coupling constant between the two nuclei results in the observation of P_A:P_B cross peaks. A considerably more *detailed* characterization of the entire $H_A-P_A-P_B-H_B$ system may be achieved by *combining* the features of an $^1H-^{31}P$ HSQC with a homonuclear $^{31}P-^{31}P$ COSY experiment, which effectively integrates the P_A:P_B COSY connectivity into the $H_{A,B}$:$P_{A,B}$ HSQC spectrum. Furthermore, a gain in sensitivity is achieved from the intrinsically high sensitivity of ^1H detection. This integration of $^1H-^{31}P$ HSQC and homonuclear $^{31}P-^{31}P$ COSY experiments is achieved by the HPP-COSY technique, whose spectral features are shown schematically in Figure 2b, c. The HPP-COSY spectrum in Figure 2b consists of the three H_A:P_A, H_B:P_B and H_C:P_C HSQC peaks, which will be referred to as "auto" peaks, in this context. The monophosphate species (H_C:P_C) shows no additional features in the spectrum. However, the $H_A-P_A-P_B-H_B$ diphosphate species exhibits two *additional* H_A:P_B and H_B:P_A "cosy" peaks, which represent a COSY pattern between the coupled P_A and P_B nuclei. Essentially, the HPP-COSY experiment facilitates magnetization transfer first between coupled ^1H and ^{31}P nuclei (HSQC) and subsequently between coupled ^{31}P nuclei (COSY). Eventually, magnetization is returned to the originating ^1H for detection. When this magnetization transfer process is achieved from either end of a $H_A-P_A-P_B-H_B$ network, the entire network may be established unambiguously.

The intensities and phases of the H_A:P_B and H_B:P_A "cosy" cross peaks are dictated by the experimental delay parameter t_{pp} (see Figure S1 in the Supporting Information). When $t_{pp} = 1/(4J_{PP})$, magnetization is transferred partially (50%) between ^{31}P nuclei in the $^{31}P-^{31}P$ COSY step, and the spectrum consists of both H_A:P_A/H_B:P_B ("auto") and H_A:P_B/H_B:P_A ("cosy") cross peaks, which are equal in intensity and opposite in phase (Figure 2b). We will refer to these spectra as HPP-4 COSY to denote the pattern of four cross peaks (two auto and two cosy) observed in an $H_A-P_A-P_B-H_B$ network (and also to reflect the $t_{pp} = 1/4J_{PP}$ delay).

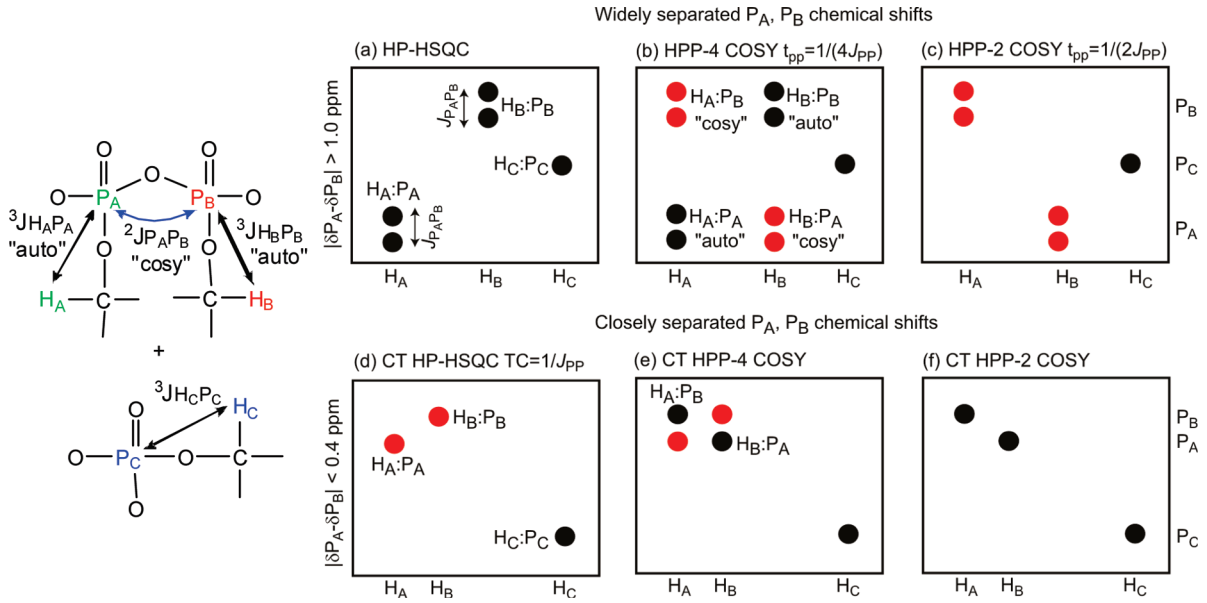

FIGURE 2. Schematic representations of HP-HSQC and HPP-COSY spectra for the $H_A-P_A-P_B-H_B$ network and an independent H_C-P_C monophosphate species. Generic structures depicting HP networks are shown on the left. Parts a–c depict situations where P_A and P_B chemical shifts are widely separated relative to the $^2J_{PP}$ coupling constant (typically, $|\delta P_A - \delta P_B| > 1.0$ ppm): (a) $^1H-^{31}P$ HSQC spectrum at high resolution, consisting of H_A:P_A, H_B:P_B ,and H_C:P_C cross ("auto") peaks. The H_A:P_A and H_B:P_B cross peaks are split into doublets due to the scalar coupling between P_A and P_B, $J_{P_AP_B}$. (b) HPP-4 COSY spectrum ($t_{pp} = 1/(4J_{PP})$) showing additional HPP-COSY ("cosy") peaks for the diphosphate species *only*. The cosy peaks H_A:P_B and H_B:P_A have opposite phase (sign) relative to the "auto" peaks H_A:P_A and H_B:P_B. (c) HPP-2 COSY spectrum ($t_{pp} = 1/(2J_{PP})$) consisting of *only* "cosy" peaks. Parts d–f depict constant time spectra of "strongly coupled" diphosphates, where the chemical shift separation between P_A and P_B is of the order of the $^2J_{PP}$ coupling constant (typically, $|\delta P_A - \delta P_B| < 0.4$ ppm). Based on typical experimental observations, H_A and H_B resonances have also been positioned close to each other. (d) Constant time (CT)-HSQC spectrum, with the experimental parameter TC (see the Supporting Information) set to $1/J_{PP}$. All species appear as singlets, with the diphosphate H_A:P_A, H_B:P_B cross peaks displaying opposite phase relative to the monophosphate H_C:P_C cross peak. (e) CT HPP-4 COSY spectrum and (f) CT HPP-2 COSY spectra demonstrating improved resolution of diphosphate peaks due to the homodecoupling effect along the ^{31}P dimension.

For $t_{pp} = 1/(2J_{PP})$, we obtain an HPP-2 COSY spectrum, which consists of *only* the two H_A:P_B and H_B:P_A cosy cross peaks in an $H_A-P_A-P_B-H_B$ network (Figure 2c). In this case, complete magnetization transfer (100%) from one ^{31}P nucleus to the other has been achieved in the $^{31}P-^{31}P$ COSY step. HPP-2 spectra are beneficial in cases where the P_A and P_B chemical shifts (and/or H_A and H_B chemical shifts) are close, leading to overcrowded HPP-4 spectra.

In many situations, there exists only a very slight difference in the chemical environments of P_A and P_B, causing their chemical shifts to be extremely close (typically, < 0.4 ppm). Typically, for the same reasons, the proton chemical shifts, H_A and H_B are also in close proximity. Under these circumstances, the diphosphate peaks are extensively overlapped leading to cancellation of auto and cosy cross peaks. In addition, strong coupling effects between P_A and P_B, are manifested as undesirable phase distortions in the peaks. As a result, the HPP-4 spectra are normally unsuitable for analysis. Although the HPP-2 spectra often perform better in terms of alleviating distortions due to strong coupling effects, these experiments do not always provide adequate resolution, owing to peak broadening as a result of the large $^2J_{PP}$ splittings. To address these situations, additional efforts are required to maximize the resolution in the ^{31}P dimension as well as to ameliorate the deleterious impact of strong coupling effects. This is achieved through the constant-time (CT) modification of HP-HSQC and HPP-COSY experiments. In CT experiments, ^{31}P doublets are effectively "homo-decoupled" and "collapse" into singlets in the ^{31}P dimension.[22,23,24,25] In this process, strong coupling effects between P_A and P_B and associated phase distortions are also suppressed significantly. The combined effects of homodecoupling of a relatively large $^{31}P-^{31}P$ coupling (typically 20 Hz) and the minimization of phase distortions result in significantly improved peak resolution and spectral quality. The schematic of a CT HP-HSQC spectrum is shown in Figure 2d. Without the CT modification, the $^2J_{PP}$ doublet splittings will prevent proper resolution of the P_A and P_B auto peaks and distortions due to strong coupling effects will lead to poor spectral quality. This advantage is carried over to CT HPP-COSY spectra, which possess the same dependence on the t_{pp} parameter as HPP-COSY spectra. Schematics of CT HPP-4 and CT HPP-2 COSY spectra are shown in parts e and f of Figure 2, respectively. It is evident from Figure 2e that the collapsing of the ^{31}P doublets in a CT HPP-4 spectrum presents a clear improvement over a simple HPP-4 COSY spectrum, in similar fashion to the CT-HSQC spectrum. However, if P_A and P_B are in extremely close proximity, then even the constant time experiment cannot avoid cancellation of auto and cosy peaks. Under these circumstances, the CT HPP-2 spectrum (Figure 2f), which

(22) Santoro, J.; King, G. C. *J. Magn. Reson.* **1992**, *97*, 202–207.
(23) Vuister, G. W.; Bax, A. *J. Magn. Reson.* **1992**, *98*, 428–435.
(24) Wu, Z.; Bax, A. *J. Magn. Reson.* **2001**, *151*, 242–252.
(25) Thrippleton, M. J.; Edden, R. A. E.; Keeler, J. *J. Magn. Reson.* **2005**, *174*, 97–109.

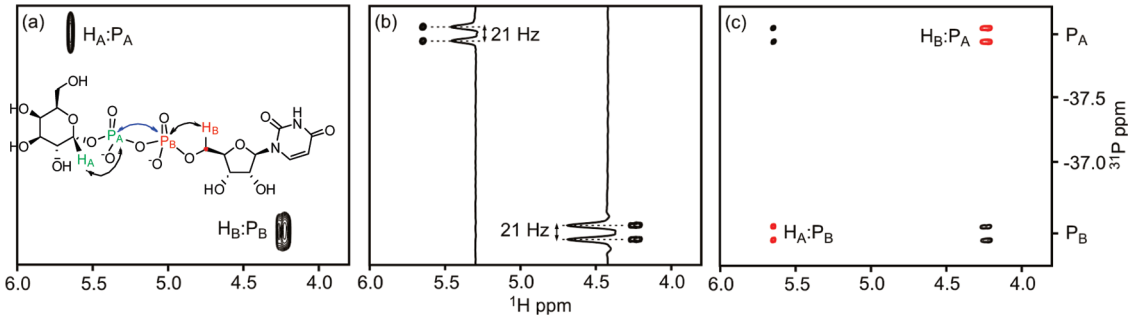

FIGURE 3. ^{1}H−^{31}P HSQC and ^{1}H−^{31}P−^{31}P COSY spectra of a 5 mM UDP-galactose (**1**) sample in D_2O at 30 °C. Only one of the two diastereotopic protons, H_B, is shown in the structure: (a) low-resolution ^{1}H−^{31}P HSQC showing the H_A:P_A and H_B:P_B correlations; (b) high-resolution ^{1}H−^{31}P HSQC showing the ^{31}P splitting due to a 21 Hz $^2J_{P_AP_B}$ coupling constant; (c) HPP-4 COSY acquired with $t_{pp} = 1/(4J_{PP})$ (13.0 ms). Both "auto" (black, H_A:P_A and H_B:P_B) and "cosy" (red, H_A:P_B and H_B:P_A) peaks are present in the spectrum (black and red represent opposite phases), demonstrating complete H_A−P_A−P_B−H_B connectivity.

consists only of cosy peaks, is the most desirable since it provides all the necessary cosy information, attenuates strong coupling artifacts, and minimizes spectral overlap. Complete connectivity in an H_A−P_A−P_B−H_B network may be obtained by overlaying independently acquired CT HSQC (Figure 2d) and CT HPP-2 (Figure 2f) spectra, without suffering from the intrinsic problems of HPP-4 or CT HPP-4 spectra.

Although CT spectroscopy is the experiment of choice for HPP spectroscopy to characterize diphosphates with closely spaced ^{31}P resonances, there is another feature of CT spectra which may be applied advantageously to *all* diphosphate containing compounds. The relative phases (signs) of mono- and diphosphate signals are dictated by the experimental delay parameter TC in HSQC experiment (see Figure S1 in the Supporting Information). When TC = $1/J_{PP}$, diphosphate resonances appear with inverted phases relative to monophosphate resonances (Figure 2d), making this a useful tool for distinguishing between the two species. This is true regardless of the magnitude of the chemical shift difference between P_A and P_B resonances, as long as they are distinct (i.e., magnetically and chemically nonequivalent). Note that it is *not* necessary to acquire a 2D spectrum to identify which protons are coupled to mono- or diphosphate species. If the detected protons are well-resolved, the phase relationship is evident from a 1D version of the CT-HSQC experiment (see Figure S2 in the Supporting Information). In two-dimensional experiments, even a low-resolution 2D spectrum can distinguish mono- and diphosphate species because the information is contained in the phases of the peaks as opposed to an HSQC spectrum, which needs to be acquired in high resolution in order to observe $^2J_{PP}$ doublets for identifying diphosphate peaks.

^{1}H−^{31}P−^{31}P COSY To Characterize Polyphosphorylated Small Molecules. UDP-galactose (1). The naturally occurring diphosphate UDP-galactose is a precursor in polysaccharide biosynthesis and is structurally related to the NDP-sugar substrates of glycosyltransferases in natural product biosynthesis. The need to synthesize and characterize NDP-sugar substrates for the study of glycosyltransferases and for glycorandomization approaches in glycosylated natural

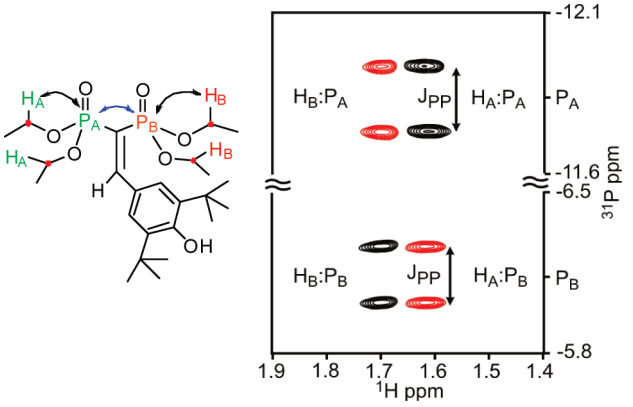

FIGURE 4. HPP-4 COSY spectrum of 5 mM **2** in C_6D_6 at 30 °C with $t_{pp} = 1/(4J_{PP}) = 5.0$ ms, illustrating the application of HPP NMR to compounds with P−C−P linkage. The "auto" (H_A:P_A and H_B:P_B) and "cosy" (H_A:P_B and H_B:P_A) peaks have opposite phase and are shown in black and red, respectively. The $H_A\cdots P_A$−C−$P_B\cdots H_B$ connectivity can be established though these peaks.

product biosynthesis[26−28] highlights NDP-sugars as important diphosphate-bearing compounds. Here, UDP-galactose represents our model for demonstrating the basic elements of HPP spectra. The H_A−P_A−P_B−H_B system is highlighted in Figure 1. Figure 3a shows an HP-HSQC spectrum of UDP-galactose, demonstrating correlations between the H_A and P_A nuclei as well as correlations between H_B and P_B nuclei. The spectrum acquired at high resolution in the ^{31}P dimension (Figure 3b) shows that each of the H_A:P_A and H_B:P_B cross peaks are split into doublets along the ^{31}P axis, due to the $^2J_{PP}$ (21 Hz) coupling constant between P_A and P_B. The fact that P_A and P_B are indeed coupled *to each other* may also be established from an HPP-4 COSY spectrum (Figure 3c) acquired with $t_{pp} = 1/(4J_{PP})$ (13.0 ms). The spectrum contains both H_A:P_A and H_B:P_B ("auto") peaks as well as phase-inverted H_A:P_B and H_B:P_A ("cosy") peaks. Note that in this example, the HPP-COSY spectrum need *not* be acquired in high resolution along the ^{31}P dimension. Since P_A and P_B exhibit a substantial chemical shift difference, "auto" and "cosy" peaks may be adequately and rapidly resolved, even in low resolution HPP-COSY spectra. From these spectra,

(26) Blanchard, S.; Thorson, J. S. *Curr. Opin. Chem. Biol.* **2006**, *10*, 263–271.

(27) Luzhetskyy, A.; Bechthold, A. *Appl. Microbiol. Biotechnol.* **2008**, *80*, 945–952.

(28) Timmons, S. C.; Thorson, J. S. *Curr. Opin. Chem. Biol.* **2008**, *12*, 297–305.

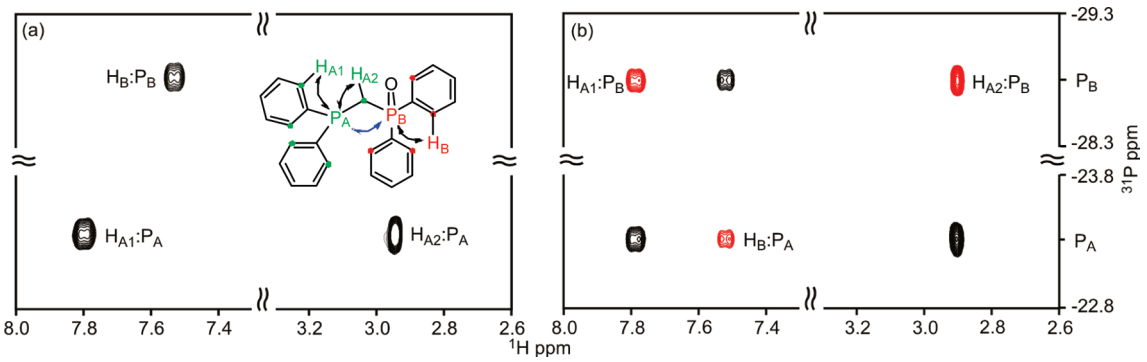

FIGURE 5. Illustration of HPP NMR applied to dppmO (**3**), a compound with a large chemical shift difference in the ^{31}P dimension. Both the ^{1}H−^{31}P HSQC (a) and HPP-4 COSY (b) spectra were taken with a 5 mM dppmO sample in C_6D_6 at 30 °C. The spectra were folded in the ^{31}P dimension to achieve high-resolution in a short time period. Auto and cosy cross peaks are evident in the spectrum shown in (b) acquired with t_{pp} set to 12.4 ms ($1/(4J_{PP})$). The "auto" peaks (black, labeled in (a)) and "cosy" peaks (red, labeled in (b)) show the $H_A-P_A-P_B-H_B$ connectivity.

the $H_A-P_A-P_B-H_B$ diphosphate linkage between the uridine and galactose components can be unambiguously established.

***P*,*P*′-[[3,5-Bis(1,1-dimethylethyl)-4-hydroxyphenyl]ethenylidene]bis-*P*,*P*,*P*′,*P*′-tetraethyl Ester (2).** Also known as SR-12813, this bisphosphonate analogue is a potent cholesterol lowering agent[29] and is distinct from UDP-galactose in that it bears a P−C−P linkage. The $H_A-P_A-P_B-H_B$ *J*-coupling network and HPP-4 COSY spectrum are shown in Figure 4. "Auto" peaks (H_A:P_A, H_B:P_B) and "cosy" peaks (H_A:P_B, H_B:P_A) are clearly observable and establish the presence of the $H_A\cdots P_A-C-P_B\cdots H_B$ connectivity. This example demonstrates the application of HPP spectroscopy for characterization of the bisphosphonate compound class bearing P−C−P linkages.

Bis(diphenylphosphine)methane Monooxide (dppmO) (3). DppmO and its analogues are versatile, widely used hemilabile ligands in organometallic chemistry.[30,31] Their effectiveness as metal ligands in catalysis arises from the presence of two phosphorus nuclei, one in the P(III) oxidation state and the other in the P(V) oxidation state, connected through a P−C−P linkage. This structural feature also renders them interesting candidates for HPP-COSY experiments, as the trivalent and pentavalent ^{31}P nuclei exhibit a large chemical shift difference. The coupling network, as outlined in Figure 1, consists of two groups of protons (H_{A1}, H_{A2}) coupled to P_A (III) and H_B coupled to P_B (V). The chemical shift difference between P_A and P_B is 52.3 ppm, corresponding to 10583 Hz at 200 MHz (^{31}P). This difference in chemical shift represents a challenge for HPP experiments, since the ^{31}P pulses in the sequence (shown in Figure S1 Supporting Information) are inadequate to cover the entire range. A modification of the pulse sequence, using composite ^{31}P pulses, proved to be effective for adequate excitation of the wider bandwidth. A comparison of the HP-HSQC and HPP-COSY spectra is shown in Figure 5a,b. Acquisition parameters are such that the ^{31}P spectral width has been reduced by a factor of ∼9, so that the two chemical shifts only appear to differ by only 6 ppm. This "folding" in the ^{31}P dimension achieves higher resolution in a shorter time period. In the HSQC spectrum, we observe $H_{A1,2}$:P_A and H_B:P_B cross peaks. Interestingly, the direct correlation between $H_{A1,2}$ and P_B is not observed, likely due to unfavorable geometry between these nuclei. However, these peaks can be observed through P_A-P_B *J* coupling using HPP-COSY spectroscopy. In the HPP-4 COSY spectrum, additional $H_{A1,2}$:P_B and H_B:P_A "cosy" crosspeaks establish the connectivity between P_A(III) and P_B(V).

Nicotinamide Adenine Dinucleotide (NAD^+) (4). NAD^+ is a common cofactor found in all living cells and is involved in a large number of biochemical redox reactions. For our studies, NAD^+ represents a particular challenge in HPP NMR: the chemical shift difference between ^{31}P nuclei in NAD^+ is small (Δppm ∼0.3) and causes a number of complications arising from resonance overlap and strong coupling effects between the two ^{31}P nuclei in the 2D spectra. The importance of employing CT-HSQC and CT-HPP-2 COSY experiments to address these complicating factors is illustrated here. In addition, we demonstrate the additional utility of CT experiments to rapidly distinguish between mono- and diphosphate moieties without the need to acquire high resolution 2D spectra.

HPP vs CT HPP Spectra. Figure 6a shows a low-resolution H−P HSQC spectrum of a mixture of NAD^+ and the monophosphate PEP. The diphosphate linkage in NAD^+ consists of $H_{A1,2}-P_A-P_B-H_{B1,2}$ as shown in Figure 6, where the two $H_{A1,2}$ protons are associated with the nicotinamide moiety and the two $H_{B1,2}$ protons with the adenosine moiety. The closely spaced $H_{A1,2}$:P_A ($\delta P_A = -36.9$ ppm) and $H_{B1,2}$:P_B peaks ($\delta P_B = -36.6$ ppm) are almost overlapping, due to the combined effects of the proximity of the P_A and P_B chemical shifts, the H_B and H_A proton resonances, and the broadening of peaks in ^{31}P due to the 20 Hz J_{PP} coupling constant. Figure 6b shows an HPP-4 COSY spectrum of NAD^+, acquired with the same resolution in the ^{31}P dimension as the HSQC spectrum in Figure 6a. Both "auto" and "cosy" peaks are severely distorted due to strong coupling effects, which are most dominant when t_{pp} is set to $1/(4J_{PP})$. In addition, the close chemical shifts in the ^{31}P dimension cause mutual extinction of the H_A:P_B and H_A:P_A cross peaks, which are opposite in phase. As a result, this experiment is clearly unsuitable for identifying HPP-COSY peaks to establish H−P−P−H connectivity in this compound.

Figure 6c shows the CT-HSQC spectrum of a mixture of NAD^+ (diphosphate) and PEP (phosphoenol pyruvate, a

(29) Berkhout, T. A.; Simon, H. M.; Pate, D. D.; Bentzen, C.; Niesor, E.; Jackson, B.; Suckling, K. E. *J. Biol. Chem.* **1996**, *271*, 14376–14382.
(30) Grim, S. O.; Satek, L. C.; Tolman, C. A.; Jesson, J. P. *Inorg. Chem.* **1975**, *14*, 656−660.
(31) Grushin, V. V. *Chem. Rev.* **2004**, *104*, 1629–1662.

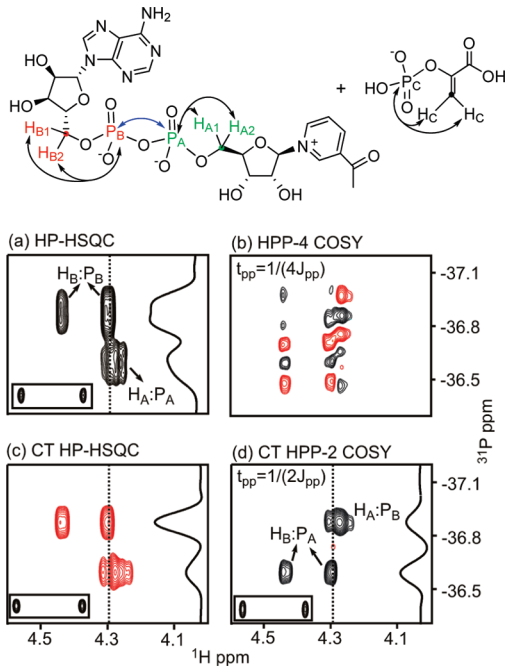

FIGURE 6. Mixture of NAD$^+$ (**4**) and monophosphate PEP (**5**) demonstrating the importance of constant time (CT) HSQC and CT HPP NMR spectra: (a) ^{1}H−^{31}P HSQC spectrum of NAD$^+$ (**4**) and PEP (**5**) showing the $H_{A1,2}$:P_A, $H_{B1,2}$:P_B correlations and peak overlap due to proximity of P_A and P_B chemical shifts, and splittings due to 20 Hz $^2J_{PP}$ couplings. PEP correlations are shown in the inset. (b) HPP-4 COSY spectrum of NAD$^+$ showing severe peak overlap of "auto" ($H_{A1,2}$:P_A and $H_{B1,2}$:P_B) and "cosy" peaks ($H_{A1,2}$:P_B and $H_{B1,2}$:P_A) accompanied by phase distortions from strong coupling effects between P_A and P_B to prevent accurate peak assignments. (c) CT-HSQC spectrum of a mixture of **4** and PEP (**5**), demonstrating resolution enhancement along the ^{31}P dimension due to collapsing of the $^2J_{PP}$ doublet into a homodecoupled singlet. This can be seen more clearly from a comparison of one-dimensional traces taken parallel to the ^{31}P axis in (a) and (c). (d) CT HPP-2 COSY spectrum exhibiting only $H_{A1,2}$:P_B and $H_{B1,2}$:P_A cosy peaks, thereby simultaneously eliminating peak overlap, enhancing resolution and sharply reducing strong coupling distortions relative to the HPP-4 spectrum in (b). Note that an overlay of (c) and (d) (see Figure S3, Supporting Information) creates a pseudo-CT HPP-4 spectrum in order to trace the $H_{A1,2}$−P_A−P_B−$H_{B1,2}$ connectivity. In the CT HSQC spectrum in (c), the $H_{C1,2}$:P_C monophosphate correlation in PEP is shown as an inset, demonstrating that the phase of the peak is opposite to that of the diphosphate peaks, thereby permitting rapid distinction between the two species.

monophosphate) (**5**) (Figure 1) obtained with TC = $1/J_{PP}$. The relevance of the PEP spectrum (shown as an inset) is explained below. Here, we focus on the NAD$^+$ diphosphate peaks. The constant time experiment collapses the $^2J_{PP}$ doublet into a singlet, thereby significantly improving the resolution of the spectrum. This is depicted in a comparison of the one-dimensional traces parallel to the ^{31}P dimension, between Figure 6a (HSQC) and c (CT HSQC). In order to correlate P_A and P_B unambiguously, the CT HPP-2 COSY spectrum was acquired (Figure 6d). As expected, it provides higher spectral quality, combining all the benefits of resolution enhancement due to the homo-decoupling effect, reduced strong coupling artifacts, and elimination of auto and cosy peak overlap.

Distinction between Mono- and Diphosphate Using CT HP-HSQC. As described above, CT HSQC spectra were acquired

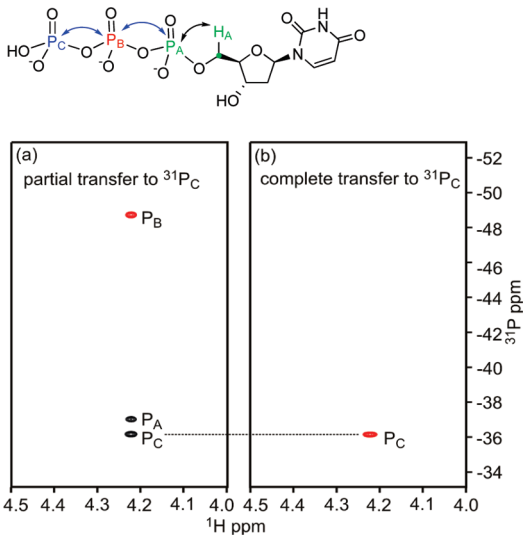

FIGURE 7. Characterization of a nucleoside triphosphate, dUTP (**6**), with the ^{1}H−^{31}P−^{31}P−^{31}P COSY experiment. The ^{1}H−^{31}P−^{31}P−^{31}P COSY spectra were acquired with two successive, "relayed" ^{31}P−^{31}P COSY elements, each with individual t_{pp} parameters. (a) H_A:P_A (auto), H_A:P_B and H_A:P_C (cosy) cross peaks obtained by setting both t_{pp} delay parameters to 1/(4J_{PP}) (12 ms). (b) H_A:P_C (cosy) cross peak obtained by setting the first t_{pp} duration to 1/(2J_{PP}) (26 ms) and the second t_{pp} duration to 1/(4J_{PP}) (12 ms).

on a mixture of NAD$^+$ (diphosphate) and PEP (phosphoenol pyruvate, a monophosphate) (**5**, Figure 1). PEP bears two protons $H_{C1,2}$ coupled to P_C. Figure 6e shows a CT-HSQC spectrum of the NAD$^+$/PEP mixture. The $H_{C1,2}$:P_C cross peaks appear significantly downfield of the NAD$^+$ peaks in the ^{31}P dimension ($\delta P_C = -22$ ppm) and are presented as an inset in Figure 6c. In the CT-HSQC spectrum, the diphosphate (NAD$^+$) peaks are of opposite phase relative to the monophosphate (PEP) peaks. Thus, this method permits rapid, unequivocal discrimination of mono- and diphosphates (as long as the diphosphate ^{31}P nuclei are magnetically nonequivalent and their chemical shifts are distinct). *Importantly, acquisition of a 2D spectrum is not always necessary to make this distinction.* If the proton resonances of the mono- and diphosphate species are distinct, a 1D CT-HSQC spectrum acquired with TC = $1/J_{PP}$ will yield opposite phases for the protons associated with mono- and diphosphates (Figure S2, Supporting Information). Even in the two-dimensional mode, where the mono- and diphosphate distinction is contained in the phases of the peaks, this information can be obtained far more quickly than an HSQC spectrum, where relatively high resolution spectra need to be acquired in order to resolve $^2J_{PP}$ doublets for identification.

Expanding HPP-COSY Techniques for the Characterization of Triphosphate Analogues. The HPP-COSY concept is easily applied to identify triphosphate moieties defined by H_A−P_A−P_B−P_C−H_C *J*-coupled networks. A simple extension involves the addition of a second, relayed COSY step to the HPP-COSY pulse sequence. The most straightforward example of a triphosphate linkage is shown in the case of dUTP (**6**, Figure 7), which exemplifies a H_A−P_A−P_B−P_C system. In this HPPP-COSY experiment, adjusting the duration (t_{pp}) of two back-to-back $P_A \rightarrow P_B$ and $P_B \rightarrow P_C$ COSY steps results in different cross peak patterns (Figure 7), which can be used to identify the triphosphate moeity. Although this was easily achievable in the case of dUTP, relayed COSY

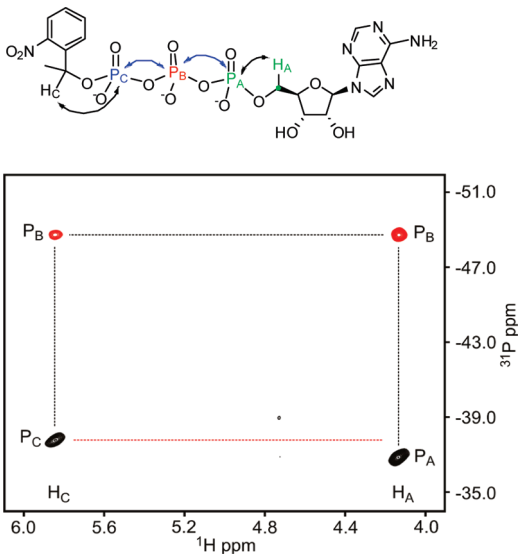

FIGURE 8. HPP-4 COSY spectrum of **7** (t_{pp} = 1/(4J_{PP}) = 11.0 ms) showing auto peaks H_A:P_A and H_C:P_C and cosy peaks H_A:P_B and H_C:P_B to demonstrate the $H_A-P_A-P_B-P_C-H_C$ connectivity. The spectrum was acquired with a sample containing 5 mM **7** in D_2O at 30 °C.

steps are not efficient when ^{31}P magnetization decays rapidly during the COSY steps. In small organic molecules, one of the most common reasons for rapid ^{31}P signal decay is exchange broadening in the presence of excess salt (as opposed to nuclear relaxation, which is more severe in large macromolecules). An example of this is demonstrated in the case of (**7**), a capped ATP analog which is used for photolysis studies, bioimaging experiments and time-resolved studies of ATP-requiring biological systems.[32,33] The $H_A-P_A-P_B-P_C-H_C$ network in this molecule is shown in Figure 1. ^{1}H−^{31}P−^{31}P−^{31}P COSY experiments attempted on the ammonium salt of this sample failed to achieve multiple $H_A\rightarrow P_A\rightarrow P_B\rightarrow P_C$ and $H_C\rightarrow P_C\rightarrow P_B\rightarrow P_A$ COSY steps. However, standard HPP-4 COSY experiments were successful in observing H_A:P_B and H_C:P_B cosy cross peaks (Figure 8), thus establishing the presence of the $H_A-P_A-P_B-P_C-H_C$ network.

A Practical Guide for Acquiring HP and HPP Spectra. To effectively adapt HPP NMR techniques to diverse situations, we have developed a systematic protocol for optimizing these experiments. An illustrated guide (Figure 9 and Figure S2, Supporting Information) to optimize HP-HSQC, CT-HP-HSQC, HPP-COSY, and CT-HPP-COSY experiments is presented below and in Figure S2 (Supporting Information).

1. If possible, obtain a ^{31}P 1D spectrum with and without ^{1}H decoupling. This yields information about ^{31}P chemical shifts and identifies ^{31}P resonances that are coupled to ^{1}H, as well as provides estimates of the J_{HP} coupling. ^{31}P−^{31}P splittings also provide information about the J_{PP} coupling constants and strong coupling effects. However, acquiring ^{31}P spectra at low concentrations (< 1 mM), is often not possible. In that case, ^{31}P chemical shifts may be inferred from typical literature values.
2. Set up a 1D HP-HSQC experiment using the pulse sequence in Figure S1 (Supporting Information). Array t_{hp} over a range of values (Figure 9b) and choose the spectrum with maximum intensity and minimum phase distortions (these arise from competing J_{HH} coupling constants, especially for geminal protons). Typical values of t_{hp} range from 10 to 40 ms.
3. Acquire a low-resolution 2D HP-HSQC spectrum (Figure 9c) and adjust the spectral width along the ^{31}P dimension if necessary. When the spectral width is very large, folding the ^{31}P dimension is recommended.
4. Set up a 1D HPP-COSY experiment to optimize the t_{pp} value (Figure 9d). Acquire 1D spectra with different values of t_{pp} and note the null (t_{pp} = 1/4J_{PP}, typically 10 to 12 ms) and the first negative maximum (t_{pp} = 1/2J_{PP}, typically 20−24 ms). (a) Acquire a 2D spectrum with t_{pp} = 1/(4J_{PP}) for compounds with large chemical shift difference in P_A and P_B. The final spectrum will have "auto" and "cosy" peaks of opposite phase. (b) Acquire a 2D spectrum with t_{pp} = 1/(2J_{PP}) for compounds with small chemical shift difference in P_A and P_B. The final spectrum will show only the "cosy" peaks.

If the spectra display severely overlapped peaks, use CT HP-HSQC and CT HPP-COSY experiments. If the relaxation losses are severe, regular HPP-COSY (without CT) should be obtained, using t_{pp} = 1/(2J_{PP}). The parameter TC can be obtained by running arrays of TC to look for the maximum inversion signal (Figure S2, Supporting Information).

Discussion

In this work, we have shown the applicability of HPP-COSY to a wide range of structurally diverse phosphorus-containing small molecules. The compounds highlighted in this study demonstrate HP-NMR characterization techniques on biologically and chemically interesting scaffolds. The basic technique was demonstrated using the model UDP-galactose, in which a characteristic HP-HSQC spectrum depicts correlations between the H_A and P_A nuclei as well as between the H_B and P_B nuclei ("auto" peaks). To establish the connectivity of uridine and galactose components through a P−O−P diphosphate linkage, the basic HSQC concept was combined with a ^{31}P−^{31}P COSY step, to generate the HPP-4 and HPP-2 experiments. In an HPP-4 COSY, a relevant experimental parameter t_{pp} is set to 1/(4 J_{PP}), resulting in the observation of a new set of "cosy" peaks correlating H_A:P_B and H_B:P_A that are opposite in phase compared to the auto peaks. The combination of the four peaks, namely; H_A:P_A (auto)/H_A:P_B (cosy) and H_B:P_B (auto)/H_B:P_A (cosy) cross peaks permit characterization of the entire $H_A-P_A-P_B-H_B$ *J*-coupled network. These experiments were also successfully applied to the bisphosphonate SR-12813, which bears a P−C−P linkage, and DppmO, a small molecule containing two ^{31}P nuclei with drastically different ^{31}P chemical shifts. In this case, ^{31}P pulses with broad excitation profiles were applied to cover the wider ^{31}P bandwidth. These latter experiments demonstrate the applicability of HPP-COSY spectroscopy to the important bisphosphonate compound class.

In contrast to UDP-galactose, SR-12813, and DppmO, close proximity of phosphorus and proton resonances in

(32) Hartung, K.; Froehlich, J. P.; Fendler, K. *Biophys. J.* **1997**, *72*, 2503–2514.
(33) Gropp, T.; Cornelius, F.; Fendler, K. *Biochim. Biophys. Acta* **1998**, *1368*, 184–200.

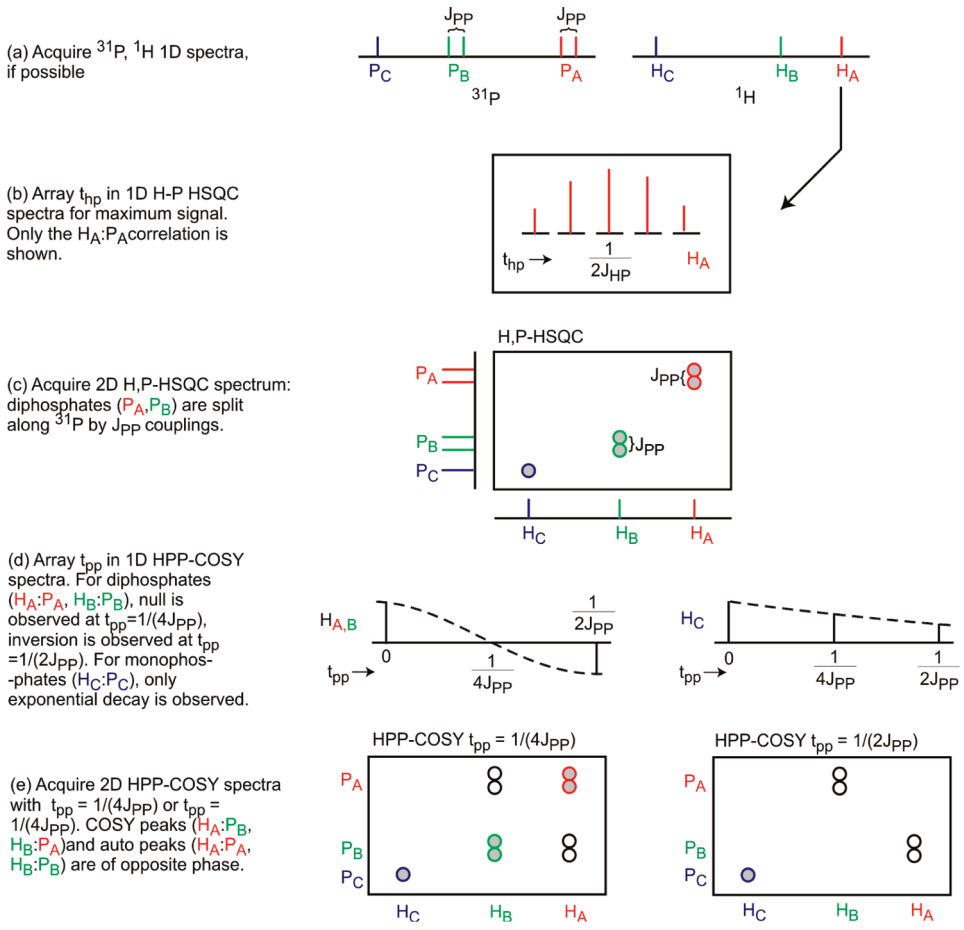

FIGURE 9. General guide for the setup of the HPP NMR experiment. The shaded peaks have opposite phase relative to the unshaded ones.

NAD^+, along with artifacts due to strong coupling between the coupled ^{31}P nuclei, resulted in near overlap of H_A:P_A and H_B:P_B auto peaks in the HSQC spectrum. This led to mutual extinction of auto and cosy cross peaks in the HPP-4 COSY. In this case, a constant time (CT) modification of HSQC spectra improved resolution by collapsing the P_A:P_B doublets into singlets and also minimized strong coupling artifacts. The CT modification was then incorporated into an HPP-2 COSY experiment ($t_{pp} = 1/(2J_{PP})$, yielding only cosy cross peaks in the spectrum, thereby resulting in considerable overall improvement in spectral quality. In addition to improving the resolution in the ^{31}P dimension by effectively homodecoupling the P−P doublets, constant time experiments permit the rapid discrimination between mono- and diphosphate resonances as a result of these species displaying resonances of opposite phase in the CT-HSQC spectrum. Thus, a mixture containing NAD^+ (diphosphate) and PEP (monophosphate) could be easily distinguished.

We have also demonstrated extensions of the HPP-COSY techniques for the characterization of triphosphate linkages in the biologically relevant triphosphate dUTP and the related masked ATP analogue **7**. In the case of dUTP, the connectivity of deoxyuridine through the P_A−O−P_B−O−P_C triphosphate linkage was easily established using the HPPP-COSY experiment which contains two successive P_A−P_B and P_B−P_C COSY steps. However, the efficiency of HPPP-COSY to establish the triphosphate linkage in the caged ATP analogue **7** was significantly reduced, likely a result of ^{31}P signal loss during the extended COSY steps, due to exchange broadening from high salt concentration in the sample. In this case, identification of the H_A−P_A−P_B−P_C−H_C network was instead accomplished through H_A:P_B and H_C:P_B obtained using a simple HPP-4 COSY experiment. Establishing connectivity to P_B from opposing molecular components of **7** effectively characterizes this triphosphate moiety.

Although HPP NMR provides an effective way to distinguish diphosphates and monophosphates in general by showing opposite phase in the CT HP-HSQC and HPP-COSY spectra of these compounds, these experiments are not suitable for detection of a bisphosphonate bearing two magnetically equivalent ^{31}P nuclei. For bisphosphonates possessing high symmetry, a simple 1D ^1H NMR, acquired with or without ^{31}P decoupling, can be used to identify the number of ^{31}P nuclei in the structure (Figure S4, Supporting Information).

Finally, we have presented a practical guide for the execution of HP and HPP NMR experiments such that these techniques can be easily implemented and effectively used as structure determination tools for the organic chemist. The examples we have discussed here, in conjunction with our previously reported application of HPP-COSY techniques to the characterization of metabolic intermediates in the MEP biosynthetic pathway, illustrate the versatility of HPP-COSY spectroscopy. When experiments are properly optimized and favorable ^{31}P relaxation conditions typical of small molecules exist, HP NMR is highly sensitive and can be applied to samples at low millimolar or submillimolar

concentrations to selectively detect and characterize phosphorylated species even in crude reaction mixtures.

Experimental Section

NMR Spectroscopy. All data were acquired on a 500 MHz (^{1}H) NMR spectrometer at 30 °C, on an "inverse detection" pentaprobe (^{1}H, ^{31}P, ^{15}N, ^{31}P, ^{2}H) equipped with actively shielded *z*-gradient coils. Data were processed with nmrPipe and analyzed using nmrDraw software.[34] All spectra were referenced with respect to triphenylphosphine oxide (TPPO) as an external standard.

Sample Preparation. The compounds used in this study are shown in Figure 1. Compounds **1**−**7** were purchased from commercial suppliers and dissolved in appropriate solvents at a final concentration of ~5 mM.

(34) Delaglio, F.; Grzesiek, S.; Vuister, G. W.; Zhu, G.; J., P.; Bax, A. *J. Biomol. NMR* **1995**, *6*, 277–293.

Acknowledgment. We acknowledge the Johns Hopkins University Biomolecular NMR center for the use of their 500-MHz NMR spectrometer. This work was supported by funding from the NIH (T32CA009243 for M.S.) and from Johns Hopkins Malaria Research Institute Pilot Grant (for C.L.F.M. and M.S.).

Supporting Information Available: Pulse sequences and some theoretical details for HPP experiments; detailed acquisition parameters for the HPP spectra shown in Figures 3−8; a figure illustrating the procedure for the optimization of the constant time HP-HSQC and HPP-COSY spectroscopy; overlay of parts c and d of Figure 6; HPP and ^{1}H 1D spectra for PEP (**5**), methylenediphosphonic acid, and zoledronic acid. This material is available free of charge via the Internet at http://pubs.acs.org